

A LATTICE MONTE CARLO STUDY OF THE HOT ELECTROWEAK PHASE TRANSITION

K. Kajantie^{a,b}, K. Rummukainen^a and M. Shaposhnikov^{a1}

^a*Theory Division, CERN,
CH-1211 Geneva 23, Switzerland*

^b*Department of Theoretical Physics, P.O.Box 9, 00014 University of Helsinki, Finland*

Abstract

We study the finite temperature electroweak phase transition with lattice perturbation theory and Monte Carlo techniques. Dimensional reduction is used to approximate the full four-dimensional SU(2) + a fundamental doublet Higgs theory by an effective three-dimensional SU(2) + adjoint Higgs + fundamental Higgs theory with coefficients depending on temperature via screening masses and mass counterterms. Fermions contribute to the effective theory only via the N_F and m_{top} dependence of the coefficients. For sufficiently small lattices ($N^3 < 30^3$ for $m_H = 35$ GeV) the study of the one-loop lattice effective potential shows the existence of the *second* order phase transition even for the small Higgs masses. At the same time, a clear signal of a *first order* phase transition is seen on the lattice simulations with a transition temperature close to but less than the value determined from the perturbative calculations. This indicates that the dynamics of the first order electroweak phase transition depends strongly on non-perturbative effects and is not exclusively related to the so-called ϕ^3 term in the effective potential.

CERN-TH.6901/93
May 1993

¹On leave of absence from Institute for Nuclear Research of Russian Academy of Sciences, Moscow 117312, Russia

1 Introduction

The interest in the study of the high temperature phase transitions in gauge theories, initiated a long time ago in [1], has been revived now in connection with possible generation of the baryonic asymmetry of the universe at the electroweak scale (see, e.g., reviews [2, 3] and references therein). The common belief, based on the perturbative calculations of the effective potential for the scalar field, is that the electroweak phase transition for moderate Higgs boson masses is weakly first order (i.e. temperature metastability range is small compared with the critical temperature). An incomplete list of references containing perturbative analysis of the phase transitions is contained in [4]-[14]. All perturbative calculations, however, work only for sufficiently large values of the scalar field, namely $\phi \gg gT$. This estimate arises as follows. Roughly speaking, there are at least three relevant mass scales at high temperatures. The first one is related to the Debye screening of the gauge charge and is of the order of $m_D = C_D gT$ (for the electroweak theory with $N_F = 6$ $C_D = \frac{11}{6}$). The second one is associated with the non-abelian magnetic sector of gauge theories, $m_M = C_M g^2 T$ (C_M is some number yet to be determined) and the third one with the gauge boson mass induced by the Higgs mechanism, $m_W = \frac{1}{2} g \phi$ with ϕ being the condensate of the scalar field. The naive loop expansion for the effective potential works well provided $m_W \gg m_D$, i.e. for $\phi \gg T$. This condition is usually not satisfied for the interesting range of fields and temperatures. The improved loop expansion which takes into account Debye mass effects in all orders of perturbation theory works for a larger interval of the scalar condensate. However, due to the infrared problem in the high temperature dynamics of gauge theories [15] any of the loop expansions break down for $m_W < m_M$ and $\phi < 2C_M gT$. Due to the fact that the coupling constant in electroweak theory is not so small ($g \approx 2/3$) it is important to know the numerical value of the coefficient C_M . If it is small, then perturbative calculations of the effective potential are valid in an interesting range of parameters, while a large value of C_M would imply the lack of any knowledge of the dynamics of the phase transition.

The appearance of the magnetic mass is a purely non-perturbative phenomenon and not a lot is known about its value. It is associated with the confinement scale of 3-dimensional gauge theory derived by dimensional reduction from 4-dimensional theory at high temperatures. Different correlation lengths in 3-dimensional SU(2) gauge theory were studied by lattice Monte-Carlo methods in [16]. It was found there that the 3-dimensional 0^{++} glueball mass (inverse screening length in this channel) is about $\sim 2g^2 T$. This indicates that non-perturbative effects are rather large and that presumably $C_M \sim 2$. If true, a perturbative analysis of the effective potential in a parameter range relevant for cosmology has low chances to remain if force after non-perturbative effects are taken into account.

In order to clarify this question, one has to use non-perturbative methods for the study of the effective potential. They are provided by lattice Monte-Carlo simulations. Some preliminary data derived with the use of 4-dimensional lattices is already available [17]-[19]. There is an indication [19] that the strength of the first order phase transition is enhanced in comparison with perturbative calculations.

The purpose of this paper is to combine perturbative and non-perturbative methods for the study of the finite T electroweak transition. Namely, with the use of dimensional reduction [20]-[24] one can first derive a 3-dimensional effective action with perturbatively calculable coefficients, summing up thus the effects of the Debye screening which are well understood. Then, one can simulate the phase transition with lattice Monte-Carlo methods.

There are a number of advantages of this method in comparison with 4-dimensional lattice simulations. First, it separates the physics in which we are reasonably confident (Debye screening) from the unknown non-perturbative 3-dimensional physics. In other words, any 4-dimensional simulations contain perturbative noise which has nothing to do with non-perturbative effects determining the order of the phase transition. Moreover, perturbation theory signals that the first order nature of the electroweak phase transition is an exclusively 3-dimensional phenomenon, since the so-called ϕ^3 term in the effective potential (this term induces a jump of the order parameter) arises due to infrared singularities in loop integrations at high temperatures. The last, but not least advantage is that a lattice simulation of 3-dimensional theories is less time consuming and more transparent from the point of view of scaling behaviour.

The paper is organized as follows. In Section 2 we derive the 3-dimensional effective action for our system. In Section 3 we compute the effective potential in the continuum 3-dimensional theory and show how the first order nature of the phase transition arises in the loop expansion of the effective potential. In Section 4 we study the effective potential for the lattice version of the theory which is then compared in Section 5 with Monte Carlo simulations. Section 6 contains our conclusions.

2 The effective action

Finite T field theoretic systems are characterised by fields defined over the interval $0 < \tau < \beta \equiv 1/T$ in imaginary time and extended beyond this region by the condition of periodicity (antiperiodicity) with the period β for bosonic (fermionic) fields. If the action is expressed in terms of the Fourier components, the quadratic terms are of the type $[(2\pi nT)^2 + \mathbf{k}^2]|A(n, \mathbf{k})|^2$, where $A(n, \mathbf{k})$ is a generic bosonic field and $n = -\infty, \dots, +\infty$. At high T and $k < 2\pi T$ the nonstatic modes $A(n \neq 0, \mathbf{k})$ are thus suppressed by the factor $(2\pi nT)^2$ relative to the static $A(0, \mathbf{k})$ modes. The idea of dimensional reduction is to exploit this suppression by integrating over the nonstatic modes in $S[A(n=0, \mathbf{k}), A(n \neq 0, \mathbf{k})]$ and deriving in this way an effective action $S_{\text{eff}}[A(0, \mathbf{k})]$ for the dominant static modes. We shall below carry this out for the four-dimensional $SU(2) +$ a fundamental Higgs theory, taking $g' = 0$ in the electroweak sector of the standard model. The effective theory then is a three-dimensional $SU(2) +$ a fundamental Higgs + an adjoint Higgs model with well defined T -dependent coefficients.

For fermionic fields the square of the inverse propagator is $[(2n+1)\pi T]^2 + \mathbf{k}^2$ and all modes are suppressed at large T . However, the fermionic fields will enter by changing the coefficients of the effective action of the bosonic static modes. Their effect can thus

also be studied in this framework. However, as our calculations so far are only on the one loop level, we can only include a top quark of mass less than 79 GeV, given by one loop stability [25].

The starting point is the action of the 4d SU(2) + fundamental Higgs model

$$S[A_\mu^a(\tau, \mathbf{x}), \phi_i(\tau, \mathbf{x})] = \int_0^\beta d\tau \int d^3x \left\{ \frac{1}{4} F_{\mu\nu}^a F_{\mu\nu}^a + (D_\mu \phi)^\dagger (D_\mu \phi) + \mu^2 \phi^\dagger \phi + \lambda (\phi^\dagger \phi)^2 \right\}, \quad (1)$$

in standard notation. Possible fermionic terms are not shown explicitly.

Including 1-loop corrections and terms not damped by powers of $1/T$ the dimensionally reduced effective action becomes

$$\begin{aligned} S_{\text{eff}}[A_i^a(\mathbf{x}), A_0^a(\mathbf{x}), \phi_i(\mathbf{x})] &= \frac{1}{T} \int d^3x \left\{ \frac{1}{4} F_{ij}^a F_{ij}^a + \frac{1}{2} (D_i A_0)^a (D_i A_0)^a + (D_i \phi)^\dagger (D_i \phi) + \right. \\ &+ \frac{1}{2} \left[\frac{2}{3} \left(1 + \frac{1}{4} + \frac{N_F}{4} \right) g^2 T^2 - (4+1) g^2 T \Sigma_c \right] A_0^a A_0^a + \frac{g^4}{12\pi^2} \left(1 + \frac{1}{16} - \frac{N_F}{8} \right) (A_0^a A_0^a)^2 + \\ &+ \left[-\frac{1}{2} m_H^2 + \left(\frac{1}{8} g^2 + \frac{1}{16} g^2 + \frac{1}{2} \lambda + \frac{g^2 m_{\text{top}}^2}{8m_W^2} \right) T^2 - \left(\frac{3}{2} g^2 + \frac{3}{4} g^2 + 6\lambda \right) T \Sigma_c \right] \phi^\dagger \phi + \lambda (\phi^\dagger \phi)^2 + \\ &\left. + \frac{1}{4} g^2 A_0^a A_0^a \phi^\dagger \phi \right\}, \end{aligned} \quad (2)$$

where Σ_c is the integral

$$\Sigma_c = \int \frac{d^3p}{(2\pi)^3 \mathbf{p}^2} \quad (3)$$

depending linearly on the cutoff. In perturbation theory it cancels against 1-loop divergences, as shown explicitly below. If one wants to study the system nonperturbatively with a finite cutoff it must be included for correct continuum limit [26]. We shall fix the parameters of the effective action by taking $g = 2m_W(\sqrt{2}G_F)^{-1/2} = 2/3$, $m_W = 80.6$ GeV and giving the value of m_H . Then $\lambda/g^2 = m_H^2/(8m_W^2)$.

The effective theory thus is a 3d SU(2) + fundamental Higgs + adjoint Higgs theory with coefficients depending on T , N_F , the coupling constants and the cutoff. All the three kinetic terms, the two $T = 0$ potential terms for ϕ and the last $A_0 - \phi$ coupling term arise from eq. (1) by naive dimensional reduction (taking fields constant in τ). The general structure of the 1-loop quadratic potential terms for A_0 and ϕ is $c_1 T^2 - c_2 T \times$ cutoff, where the first term is the usual 4d 1-loop screening mass and the second term arises from the exclusion of the $n = 0$ term in the 1-loop integral (since one must only integrate over the nonstatic modes). Equivalently, this term is the mass counterterm of the superrenormalisable 3d theory. The contributions of the various fields to these terms in eq. (2) are ordered so that in the coefficient of $\phi^\dagger \phi$ first come the terms with A_i^a in the loop, then A_0 , then ϕ and last the fermion loop (only in the T^2 terms). In the quadratic and quartic A_0 terms the ordering is A_i^a , ϕ , fermions in the loop. The A_0 loop gives a contribution of order g^4 and is neglected here. Also neglected are small 1-loop corrections to the quartic ϕ term.

In addition to the mass counterterm eq. (3) there in 3d actually also is [26] a logarithmic 2-loop counterterm $\sim \lambda^2 T^2 / (16\pi^2) \int dp / |\mathbf{p}|$. This is numerically negligible in our case.

More generally, eq. (2) contains terms with higher powers of fields and their derivatives, allowed by the gauge (BRS) invariance of the 3d theory. For example, the term $g^6(A_0^a A_0^a)^3/T^2$ would appear. If we take the correlation length of the A_0 field to be $1/(gT)$ we can estimate from the quadratic term that $\langle A_0^a A_0^a \rangle \sim gT^2$. Thus the ratio of terms with consecutive powers of $A_0^a A_0^a$ is $\mathcal{O}(g^3) \ll 1$.

3 The one-loop effective potential in continuum.

To study the theory defined by the action eq. (2) in perturbation theory, we compute the 1-loop correction $V_{1\text{loop}}(\phi, A_0)$ to the tree potential defined by eq. (2). One finds before regularisation that

$$\begin{aligned}
V_{1\text{loop}}(\phi, A_0) = T \int \frac{d^3 p}{(2\pi)^3} & \left\{ 2 \log(\mathbf{p}^2 + g^2 A_0^2 + \frac{1}{4} g^2 \phi^2) + \log(\mathbf{p}^2 + \frac{1}{4} g^2 \phi^2) + \right. \\
& + \frac{3}{2} \log(\mathbf{p}^2 + \mu^2 + \lambda \phi^2 + \frac{1}{4} g^2 A_0^2) + \log(\mathbf{p}^2 + m_D^2 + \frac{1}{4} g^2 \phi^2 + \lambda_A A_0^2) + \\
& + \frac{1}{2} \log\{\mathbf{p}^4 + \mathbf{p}^2[\mu^2 + m_A^2 + (3\lambda + \frac{1}{4} g^2)\phi^2 + (\frac{1}{4} g^2 + 3\lambda_A)A_0^2] + \\
& \left. + (\mu^2 + 3\lambda\phi^2 + \frac{1}{4} g^2 A_0^2)(m_D^2 + \frac{1}{4} g^2 \phi^2 + 3\lambda_A A_0^2) - \frac{1}{4} g^4 A_0^2 \phi^2\} \right\}, \tag{4}
\end{aligned}$$

where $\phi^2 = 2\phi^\dagger\phi$ and $A_0^2 = A_0^a A_0^a$. The first two terms come from the A_i loop and the remaining ones from the coupled A_0, ϕ loops. Using

$$\int \frac{d^3 p}{(2\pi)^3} \log[\mathbf{p}^2 + \mu^2 + m^2(\phi)] = m^2(\phi)\Sigma_c - \frac{1}{6\pi}[\mu^2 + m^2(\phi)]^{3/2} \tag{5}$$

one finds that the Σ_c terms in eq. (2) and eq. (5) cancel (taking into account the A_0 loop term $-\frac{1}{2}5\lambda_A T\Sigma_c A_0^2$ neglected in eq. (2) for smallness). The finite terms give the quantum correction to the tree potential. The resulting 1-loop improved potential is then

$$\begin{aligned}
V(\phi, A_0) &= \frac{1}{2}\mu^2\phi^2 + \frac{1}{2}m_D^2 A_0^2 + \frac{1}{4}\lambda(\phi^2)^2 + \frac{1}{4}\lambda_A(A_0^2)^2 + \frac{1}{8}g^2 A_0^2 \phi^2 - \\
& - \frac{T}{6\pi} \left\{ 2g^3(\frac{1}{4}\phi^2 + A_0^2)^{3/2} + \frac{1}{8}g^3\phi^3 + \right. \\
& + (m_D^2 + \frac{1}{4}g^2\phi^2 + \lambda_A A_0^2)^{3/2} + \frac{1}{2}(m_D^2 + \frac{1}{4}g^2\phi^2 + 3\lambda_A A_0^2)^{3/2} + \\
& \left. + \frac{3}{2}(\mu^2 + \lambda\phi^2 + \frac{1}{4}g^2 A_0^2)^{3/2} + \frac{1}{2}(\mu^2 + 3\lambda\phi^2 + \frac{1}{4}g^2 A_0^2)^{3/2} \right\}, \tag{6}
\end{aligned}$$

where

$$\mu^2 = \gamma(T^2 - T_0^2), \quad \gamma = \frac{3}{16}g^2 + \frac{1}{2}\lambda + \frac{g^2 m_{\text{top}}^2}{8m_W^2}. \tag{7}$$

We have, for completeness included the small λ_A term, which will again be neglected from now on.

Studying the minima of $V(\phi, A_0)$ one sees that they can be driven to nonzero values of A_0 only if the negative term is large. This demands that at least $g > \pi\sqrt{8/3}$ which is beyond the domain of validity of this calculation. We conclude that the minimum is always at $A_0 = 0$; no condensate is formed. Basically this is due to the large value of m_D and the small value of the correction, $\sim -T/6\pi$.

For $A_0 = 0$ and $\lambda \ll g^2$ the corrections to the effective potential have the form

$$\delta V = -\frac{g^3}{16\pi}T\phi^3 - \frac{T}{4\pi}(m_A^2 + \frac{1}{4}g^2\phi^2)^{\frac{3}{2}}. \quad (8)$$

It is the first term which gives rise to the first order phase transition in perturbation theory. Note that the effective 3-dimensional theory correctly takes into account Debye screening, which decreases the magnitude of the cubic term relative to the naive loop expansion by the factor $2/3$ [9]. The second term corrects the γ in eq. (7) by the term $(-3/16\pi)\sqrt{2/3}g^3$. With this input the equation

$$\frac{m_H^2}{4T_0^2} = \frac{g^2}{2} \left(\frac{3}{16} + \frac{1}{2} \frac{m_H^2}{8m_W^2} + \frac{m_{\text{top}}^2}{8m_W^2} - \frac{\sqrt{3}}{8\pi\sqrt{2}}g \right) = \frac{m_H^2}{4T_c^2} + \frac{g^4}{32\pi^2} \frac{m_W^2}{m_H^2} \quad (9)$$

gives the perturbative result for the transition temperature T_c and the lower end $T_0 < T_c$ of the metastability range (the high T phase does not exist for $T \leq T_0$). Numerical values for these as well as for some other relevant quantities as calculated from 1-loop perturbation theory [7], [10] are given in Table 1. For $g = 2/3$ the relevant formulas are $\xi(T_c)T_c = 9\pi m_H/m_W$, $T_c/m_W(T_c) = 9\pi m_H^2/(2m_W^2)$, $\sigma/T_c^3 = 2m_W^5/(243\pi^3 m_H^5)$, $L/T_c^4 = 2m_W^4[1/6 + m_H^2/(18m_W^2) - m_W^2/(18\pi^2 m_H^2)]/(9\pi^2 m_H^4)$.

m_H	T_0	T_c	T_+	$\xi(T_c)$	$m_W^{-1}(T_c)$	σ	L
35	90.89	95.24	95.83	$12.28/T_c$	$2.67/T_c$	$0.017T_c^3$	$0.085T_c^4$
80	182.34	183.55	183.71	$28.1/T_c$	$13.9/T_c$	$0.00028T_c^3$	$0.0044T_c^4$

Table 1: Values of T_c , the lower (T_0) and upper (T_+) ends of the metastability range, the correlation length ξ for the Higgs field at $T = T_c$, the gauge field correlation length $1/m_W(T_c)$, the interface tension σ and the latent heat L as calculated from 1-loop perturbation theory for $m_H = 35$ and 80 GeV, for $g = 2/3$ and for no fermions included.

4 The lattice action and effective potential.

4.1 Lattice action.

To latticeize eq. (2) we go over to the matrix representation $A_0 = A_0^a T^a$, $T^a = \frac{1}{2}\sigma_a$, $\phi \rightarrow \Phi = (\phi_0 + i\sigma_i\phi_i)/\sqrt{2}$ and rescale the fields by

$$igaA_0 \rightarrow A_0, \quad \Phi \rightarrow \sqrt{\frac{T}{a}} \frac{\beta_H}{2} \Phi, \quad (10)$$

where a is the lattice spacing. The lattice action on an N^3 lattice then becomes

$$\begin{aligned}
S = & \beta_G \sum_x \sum_{i < j} (1 - \frac{1}{2} \text{Tr } P_{ij}) + \\
& + \frac{1}{2} \beta_G \sum_x \sum_i [\text{Tr } A_0(\mathbf{x}) U_i^{-1}(\mathbf{x}) A_0(\mathbf{x} + i) U_i(\mathbf{x}) - \text{Tr } A_0^2(\mathbf{x})] + \\
& + \sum_x \left\{ 10 \Sigma(N^3) - \frac{5 + N_F}{3} \frac{4}{g^2 \beta_G} \right\} \frac{1}{2} \text{Tr } A_0^2(\mathbf{x}) + \\
& + \sum_x \frac{g^2 \beta_G}{3\pi^2} (1 + \frac{1}{16} - \frac{N_F}{8}) (\frac{1}{2} \text{Tr } A_0^2(\mathbf{x}))^2 + \\
& + \beta_H \sum_x \sum_i [\frac{1}{2} \text{Tr } \Phi^\dagger(\mathbf{x}) \Phi(\mathbf{x}) - \frac{1}{2} \text{Tr } \Phi^\dagger(\mathbf{x}) U_i(\mathbf{x}) \Phi(\mathbf{x} + i)] + \\
& + \sum_x [(1 - 2\beta_R - 3\beta_H) \frac{1}{2} \text{Tr } \Phi^\dagger(\mathbf{x}) \Phi(\mathbf{x}) + \beta_R (\frac{1}{2} \text{Tr } \Phi^\dagger(\mathbf{x}) \Phi(\mathbf{x}))^2] + \\
& - \frac{1}{2} \beta_H \sum_x [\frac{1}{2} \text{Tr } A_0^2(\mathbf{x}) \frac{1}{2} \text{Tr } \Phi^\dagger(\mathbf{x}) \Phi(\mathbf{x})],
\end{aligned} \tag{11}$$

where

$$\Sigma(N^3) = \frac{1}{4N^3} \sum_{n_i=0}^{L-1} \frac{1}{\sin^2(\pi n_1/N) + \sin^2(\pi n_2/N) + \sin^2(\pi n_3/N)} \tag{12}$$

(the term with all $n_i = 0$ is omitted; numerically $\Sigma(N^3) = 0.224605, 0.233942, 0.238633, 0.243326, 0.252731$ for $N = 8, 12, 16, 24, \infty$, respectively) and

$$\begin{aligned}
\beta_G &= \frac{4}{g^2 T a} \\
\beta_R &= \frac{1}{4} \lambda T a \beta_H^2 = \frac{m_H^2}{8m_W^2} \frac{\beta_H}{\beta_G} \\
\mu^2(T) &= \frac{2(1 - 2\beta_R - 3\beta_H)}{\beta_H a^2}.
\end{aligned} \tag{13}$$

In eq. (13) $\mu^2(T)$ is the coefficient of the $\phi^\dagger \phi$ term in eq. (2) with the continuum Σ_c replaced by $\Sigma(N^3)/a$. Introducing this relates β_H and T for given values of g, m_W, m_H (and possibly of m_{top}):

$$\frac{m_H^2}{4T^2} = \left(\frac{g^2 \beta_G}{4} \right)^2 \left[3 - \frac{1}{\beta_H} + 2 \frac{m_H^2}{8m_W^2} \frac{\beta_H}{\beta_G} - \frac{9}{2\beta_G} (1 + \frac{m_H^2}{3m_W^2}) \Sigma(N^3) \right] + \frac{g^2}{2} \left(\frac{3}{16} + \frac{1}{2} \frac{m_H^2}{8m_W^2} + \frac{m_{\text{top}}^2}{8m_W^2} \right), \tag{14}$$

The curve $T = T(\beta_H)$ is plotted in Fig.1 for a few parameter values. The curves shift to the right (left) with increasing m_H and $\Sigma(N^3)$ (β_G). For example, the values of β_H corresponding to $T = T_0$ and $T = \infty$ are

$$\beta_H(T_0) = \frac{1}{3} + (1 + \frac{m_H^2}{3m_W^2}) \frac{\Sigma(N^3)}{\beta_G} + \mathcal{O}(\beta_G^{-2}), \quad \beta_H(T = \infty) = \beta_H(T_0) - \frac{m_H^2}{108\beta_G m_W^2}. \tag{15}$$

Eq.(14) takes correctly into account the divergent mass counterterms of the 3d theory. In addition to these, there will be finite renormalisations of the coupling constants g and λ . Due to infrared divergences getting more and more serious at higher orders [27] these renormalisations – which will depend on the lattice size N – cannot be calculated perturbatively. We shall observe that the numerical results will follow the ”constant physics” curve eq. (14), with N dependent mass renormalisation but N independent bare values of g and λ , rather well. However, some more N dependence, clearly attributable to finite renormalisations of the coupling constants, will remain. In any case, all finite size effects will be very difficult to control. For example, it is not known how to include the constant mode (the $n_i = 0$ term in eq. (12)) term in perturbative calculations.

4.2 Effective potential on the lattice.

Monte-Carlo lattice simulations should be compared with the perturbative calculations of the effective potential on the lattice rather than with continuum expressions. To get a lattice generalization for the effective potential one can just change the integration over momenta in eq. (5) to a finite sum over the discrete momenta $p_i = (2\pi/aN)n_i$, $n_i = 0, \dots, N-1$. Including only the A_i loop term, which is relevant for the first order nature of the transition, the lattice effective potential becomes

$$V_{\text{latt}} = \frac{1}{2}\gamma(T^2 - T_0^2)\phi^2 + \frac{1}{4}\lambda\phi^4 + \frac{3T}{(aN)^3} \sum_{n_i=0}^{N-1} \left[\log\left(1 + \frac{(ga\phi/4)^2}{d}\right) - \frac{(ga\phi/4)^2}{d} \right], \quad (16)$$

where

$$d = \sin^2(\pi n_1/N) + \sin^2(\pi n_2/N) + \sin^2(\pi n_3/N). \quad (17)$$

Note that in this sum the term with $n_i = 0$ must not be included not only since we cannot handle it but also by definition since the effective potential is constructed for x -independent ϕ and thus constant ϕ configurations must not be integrated over.

To study the order of the transition it is convenient to study the zeroes of

$$\frac{dV_{\text{latt}}}{\phi d\phi} = \gamma(T^2 - T_0^2) + \lambda\phi^2 - \frac{3g^4}{128}\phi^2 aT \frac{1}{N^3} \sum_{n_i=0}^{N-1} \frac{1}{d[d + (ga\phi/4)^2]}, \quad (18)$$

In the continuum limit $a \rightarrow 0$, $N \rightarrow \infty$, $aN \rightarrow \infty$ the last term becomes $-(3/16\pi)g^3T\phi$. For $T = T_0$ one then is solving $\lambda\phi^2 - (3/16\pi)g^3T\phi = 0$, which trivially leads to a second minimum. This also exists for some temperatures above T_0 , up to $T = T_+$. The case of finite lattices is completely different. It is clear from the lattice expression for the effective potential that it is an analytic function of ϕ^2 at least for $\phi^2 < (16/g^2a^2)\sin^2(\pi/N)$ and, therefore, no term $\sim -\phi$ can appear. Nevertheless, a second minimum can exist for sufficiently large lattice sizes. The condition for this simply is that the equation

$$\lambda = \frac{3g^4}{128}aT \frac{1}{N^3} \sum_{n_i=0}^{N-1} \frac{1}{d[d + (ga\phi/4)^2]} \quad (19)$$

have a solution. The right hand side decreases monotonically when ϕ increases and we can take $\phi = 0$; if a solution appears it appears first at $\phi = 0$. Inserting $aT = 4/(g^2\beta_G)$ and $\lambda = g^2m_H^2/(8m_W^2)$ gives the relation

$$\frac{4}{3}\beta_G \frac{m_H^2}{m_W^2} = \frac{1}{N^3} \sum_{n_i=0}^{N-1} \frac{1}{d^2} \approx 0.17N. \quad (20)$$

The approximation is the result of an explicit numerical calculation of the sum. For the value $\beta_G = 20$ used in our numerical simulations one sees that for $m_H = 35$ GeV a first order transition appears for $N > 29$ and for $m_H = 80$ GeV for $N > 160$. The use of so large lattice volumes is not possible in practice, and we at this stage confined ourselves to smaller N , $N \leq 20$. If perturbation theory works well, one should not find any signal of a first order phase transition in the Monte-Carlo simulations with these small lattices.

It may be of interest to note that in the limit of large lattices ($a = \text{constant}$, $N \rightarrow \infty$) the last term in eq. (16) can be written in the form [29]

$$\frac{3T}{a^3} \int_0^\infty dy \left[\frac{1}{y} (1 - \exp[-(ga\phi/4)^2 y]) - (ga\phi/4)^2 \right] \exp(-3y) I_0^3(y), \quad (21)$$

with the aid of the Bessel function I_0 . Numerically this is very close to the continuum result, in particular, the $\phi \rightarrow 0$ limits are the same. In other words, the critical temperature as well as the metastability range given in Table 1 are practically the same for very large N and for the continuum.

5 Lattice simulations

Our choice of parameters for the simulations is motivated as follows. We have already fixed that $g = 2/3$ and $m_W = 80.6$ GeV. Since our aim is to test the validity of perturbation theory we choose $m_H = 35$ GeV, which makes λ small = 0.0105 but is not too close to the vacuum stability limits of somewhat less than 10 GeV. For comparison we also choose $m_H = 80$ GeV ($\lambda=0.0547$). We also do not expect fermions (except perhaps for the top quark) to qualitatively change the nature of the transition and thus choose $N_F = 0$. Light fermions could simply be included by changing the numerical value of the coefficients as in eq. (2). Finally, we choose $\beta_G = 20$, which basically fixes the lattice spacing a in physical units via the first equation in eq. (13): $a = 0.45/T$. As should, this is smaller than the thermal distance scale $1/T$, the average distance between particles. Equivalently, in order to describe correctly effects associated with magnetic sector of the 4-dimensional theory one must have $a \ll 1/m_M$. With the use of $C_M \approx 2$ and $\beta_G = 20$ we get $a \approx 0.5/m_M$. For this a the perturbative Higgs field correlation lengths in Table 1 are $27a$ ($m_H = 35$) and $42a$ ($m_H = 80$) while the gauge field correlation lengths are $6a$ ($m_H=35$) and $14a$ ($m_H = 80$). These are so large that it is realistically not possible to fit an interface between two phases (broken and unbroken) in the lattice.

5.1 The update algorithm.

Because the lattice system described by the action eq. (11) has several qualitatively different components, we used a wide mixture of update algorithms to obtain good performance. The SU(2) gauge field was updated as follows: first, we combined the plaquette action (first term in eq. (11)) and the Φ -field hopping term (fifth term) to form a local SU(2) action of the form $\beta_i^{\text{eff}}(x)\text{Tr} X_i(x)U_i(x)$, $X \in \text{SU}(2)$. Using this action, new link matrices were generated with the Kennedy-Pendleton heat bath method [28]. The adjoint field hopping action $S_{\text{hopp}}(U, A_0)$ (second term), which is quadratic in U_i , was then taken into account by accepting or rejecting the new link matrices with the Metropolis method – that is, with the condition $\exp[S_{\text{hopp}}(U^{\text{new}}, A_0) - S_{\text{hopp}}(U^{\text{old}}, A_0)] > r$, where r is a random number from an uniform distribution between 0 and 1. The acceptance rate for the Kennedy-Pendleton heat bath was $\sim 99.5\%$ and for the accept/reject step $\sim 95\%$.

The length of the adjoint field $R_A = (A_0^a A_0^a)^{1/2}$ was updated with the Metropolis method, while the colour space direction, which appears only in the hopping term, was updated with an SO(3) heat bath. Similarly, the fundamental Higgs field was divided into radial and SU(2) parts: $\Phi = RV$, $R > 0$, $V \in \text{SU}(2)$. The V -field, which appears only in the hopping term (the fifth term in eq. (11)), was updated with the Kennedy-Pendleton heat bath algorithm, and the length R was updated with the Metropolis algorithm.

The evolution of the gauge and A_0 -fields in the simulation time was very rapid compared to the evolution of the Φ -field. It is crucial to make the Higgs field update as effective as possible. Because of the large β_G the gauge background of the Higgs field is very flat, and it is plausible that one could construct an effective multigrid or cluster update algorithm.

5.2 The results.

Results of the simulations are shown in Figs. 2-6. In Fig.2 we present the probability distribution of the order parameter $L = \text{Tr} V^\dagger(\mathbf{x})U_i(\mathbf{x})V(\mathbf{x} + i)$ for $m_H = 35$ GeV and different lattice sizes. The two peak structure characteristic of a first order phase transition is clearly seen on these 8^3 and 20^3 lattices, as well as on intermediate 12^3 and 16^3 lattices (not shown). The change of the curves with the lattice volume is qualitatively consistent with what one would expect from a first order transition, namely the two peak structure is more distinguished on the large lattices. Note that the peak positions do not depend on the lattice size which indicates that the finite volume effects are not substantial.

The first order nature of the phase transition can be also seen in Fig. 3 where the simulation time evolution of the order parameter L is shown. Here initially the system was confined in the unbroken phase with small value of L , then it jumps to the phase with broken symmetry and stays there quite a long time. These jumps then continue in Monte Carlo "time".

An important criterion for the order of the phase transition is the finite size scaling

of the second moment of the order parameter L [30]. This is shown on Fig. 4 for various lattice sizes. The continuous curves were obtained by combining the individual runs (performed at various β_H 's) with the multiple histogram (Ferrenberg-Swendsen) method [31]. We observe that the second moment of L , as a function of β_H , develops a narrow peak as the volume is increased. The height and the location of the peak have well-defined infinite volume limits; this behaviour is characteristic for systems exhibiting a first order phase transition.

Analogous data for a more heavy Higgs ($m_H = 80$ GeV) is presented on Figs. 5-6. In this case the correlation lengths for the Higgs and W bosons are larger than the lattice size and strong volume dependence is observed (Fig. 6). No definite conclusion can be made for this case with the present lattice sizes.

According to Fig.2 the transition for $m_H = 35$ GeV takes place at about $\beta_H = 0.34010$ roughly independent of the lattice size. We thus do not observe precise scaling according to eq. (14), which would demand that the value corresponding to some fixed temperature change according to eq. (15) with lattice size N . We ascribe this to the nonperturbative renormalisations of g and λ discussed above. If we extrapolate to the curve corresponding to $N = \infty$, we see that $\beta_H = 0.34010$ corresponds to $T_c \approx 85$ GeV, somewhat but not much below the continuum perturbative value of $T_c = 95$ GeV. For $m_H = 80$ GeV the results are less conclusive, but for the largest lattice studied the transition takes place at $\beta_H = 0.3418$. The m_H dependence of eq. (15) is rather well reproduced, but so far it is impossible to make a definite conclusion concerning N dependence. Anyway it is suggested by Fig.1 that again the T_c observed is less than the perturbative value of 184 GeV.

6 Conclusions

We have performed a combined analytical and numerical study of the finite T electroweak phase transition. First those degrees of freedom which – with reasonable degree of confidence – can be treated perturbatively were analytically integrated over and an effective action in the remaining degrees of freedom was derived. This effective theory is a $T = 0$ 3d SU(2) gauge field + adjoint Higgs + fundamental Higgs theory with known coefficients depending on T and, quite essentially, on the cutoff of the theory. This bare effective theory was then latticized with $1/a$, $a =$ lattice spacing, as the cutoff and the nonperturbative degrees of freedom were treated numerically with Monte Carlo techniques.

In this first numerical application our aim was to study the structure of the theory and a fairly small Higgs mass, $m_H = 35$ GeV was mainly discussed, with some results given also for $m_H = 80$ GeV. A first order transition was clearly seen at least for the smaller Higgs mass and the numerical value of T_c is rather close to (but less than) the value obtained from 1-loop perturbation theory. For this numerical agreement the computable cutoff dependence of the bare effective theory was crucial. With increasing m_H the various characteristic lengths in the problem increase rapidly and the problem becomes numerically more and more difficult.

Our lattice Monte Carlo results thus clearly indicate that there is a first order phase transition, at least for small values of the Higgs mass. A very intriguing part of the result is that we see a *first order* phase transition also on *small* lattices where, according to the perturbative calculations in Section 4.2, the phase transition must be of the second order. A number of tests including the lattice volume dependence of the order parameter, temperature metastability range, etc. indicate that the first order character of the phase transition is not a lattice artifact. These results indicate that so-called ϕ^3 term is *not* the only source for the first order character of the electroweak phase transition and that non-perturbative effects are important as well. The physical nature of these non-perturbative effects should be presumably related to the confinement in 3-dimensional gauge theory. Unfortunately, the complete solution of the problem of the electroweak phase transition by non-perturbative lattice methods requires huge lattices.

Acknowledgment

The authors are grateful to K. Farakos for the collaboration at the initial stage of this work and providing us his code for 3-dimensional simulations of 3-dimensional gauge theory with a Higgs doublet.

References

- [1] D. A. Kirzhnits, JETP Lett. 15 (1972) 529;
D. A. Kirzhnits and A. D. Linde, Phys. Lett. 72B (1972) 471
- [2] M. Shaposhnikov, In: 1991 Summer School in High Energy Physics and Cosmology, v. 1, p. 338, World Scientific, 1992;
N.Turok, Preprint IMPERIAL-TP-91-92-33, 1992;
D.B.Kaplan, A.G.Cohen and A.E.Nelson, Preprint UCSD-PTH-93-02/BUHEP-93-4, 1993
- [3] G. R. Farrar and M. E. Shaposhnikov, Preprint CERN-TH.6734/RU-93-11, 1993
- [4] D.A.Kirzhnits and A.D.Linde, Ann. Phys. 101 (1976) 195;
A.D.Linde, Nucl. Phys. B216 (1983) 421, Rep. Prog. Phys. 47 (1984)925
- [5] K. Takahashi, Phys. Rev. Lett. 56 (1986) 7
- [6] M. E. Shaposhnikov. Nucl. Phys. B287 (1987) 757; A. I. Bochkarev and M. E. Shaposhnikov, Mod. Phys. Lett. 2A (1987) 417
- [7] G. W. Anderson and L. J. Hall, Phys. Rev. D45 (1992) 2685
- [8] M. Carrington, Phys. Rev. D45 (1992) 2933
- [9] M. Dine, R.G. Leigh, P. Huet, A. Linde and D. Linde, Phys. Rev. D46 (1992) 550

- [10] K. Enqvist, J. Ignatius, K. Kajantie and K. Rummukainen, Phys. Rev. D45 (1992) 3415
- [11] D.E.Brahm, C.G.Boyd and S.D.H Hsu. Preprint EFI-92-22, 1992
- [12] P.Arnold and E.Espinosa, Preprint UW/PT-92-18, 1992
- [13] M.Quiros, J.R.Espinosa and F. Zwirner, Preprint CERN-TH.6577/92, 1992
- [14] W. Buchmüller, Z. Fodor, T. Helbig and D. Walliser, Preprint DESY 93-021, 1993
- [15] A.D. Linde, Phys. Lett. 96B (1980) 289;
D. Gross, R. Pisarski and L. Yaffe, Rev. Mod. Phys. 53 (1981) 43
- [16] A. Irbäck and C. Peterson, Phys. Lett. 174B (1986) 99;
G. Koutsoumbas, K. Farakos and S. Sarantakos, Phys. Lett. 189B (1986) 173
- [17] P. H. Damgaard and U. M. Heller, Phys. Lett. B171 (1986) 442
- [18] H.G.Evertz, J. Jersák and K. Kanaya, Nucl. Phys. B285 (1987) 229
- [19] B. Bunk, E.-M. Ilgenfritz, J. Kripfganz, A. Schiller, Phys. Lett. B284 (1992) 371;
Bielefeld Preprint BI-TP 92/46
- [20] S. Nadkarni, Phys. Rev. D27 (1983) 917; Phys. Rev. D38 (1988) 3287
- [21] P. Ginsparg, Nucl. Phys. B170 (1980) 388
- [22] N. P. Landsman, Nucl. Phys. B322 (1989) 498
- [23] T. Reisz, Z. Phys. C53 (1992) 169
- [24] P. Lacock, D. Miller and T. Reisz, Nucl. Phys. B369 (1992) 501
- [25] N. V. Krasnikov, Yad. Fiz. 28 (1978) 549;
H. D. Politzer and S. Wolfram, Phys. Lett. 82B (1979) 242
- [26] G. Parisi, Statistical Field Theory, Addison Wesley 1988, Ch. 5
- [27] R. Jackiw and S. Templeton, Phys. Rev. D23 (1981) 2291
- [28] A. D. Kennedy and B. J. Pendleton, Phys. Lett. 155B (1985) 393
- [29] H.-T. Elze, K. Kajantie and J. Kapusta, Nucl. Phys. B304 (1988) 832
- [30] C. Borgs, R. Kotecký and S. Miracle-Sole, J. Stat. Phys. 62 (1991) 529
- [31] A. M. Ferrenberg and R. H. Swendsen, Phys. Rev. Lett. 61 (1988) 2635

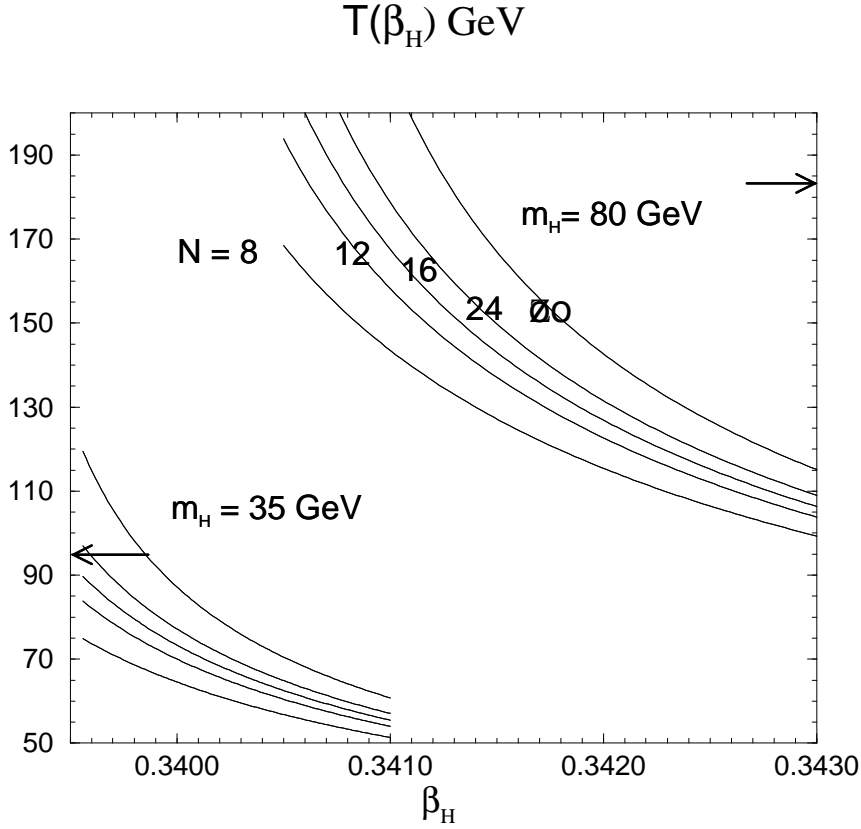


Figure 1: The relation between T and β_H as given by eq. (14) for $m_H = 35$ and 80 GeV, $\beta_G = 20$ and $N_F = 0$. The arrows denote the perturbative values of T_c as given in Table 1.

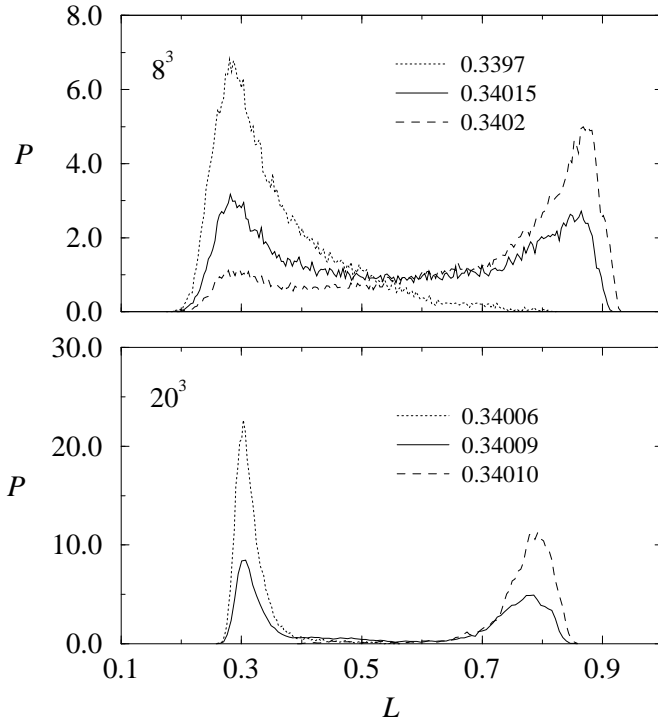


Figure 2: The distribution of $L = \text{Tr} V^\dagger(\mathbf{x}) U_i(\mathbf{x}) V(\mathbf{x} + i)$ for $m_H = 35$ GeV for 8^3 and 20^3 lattices for $\beta_G = 20$ and different values of β_H .

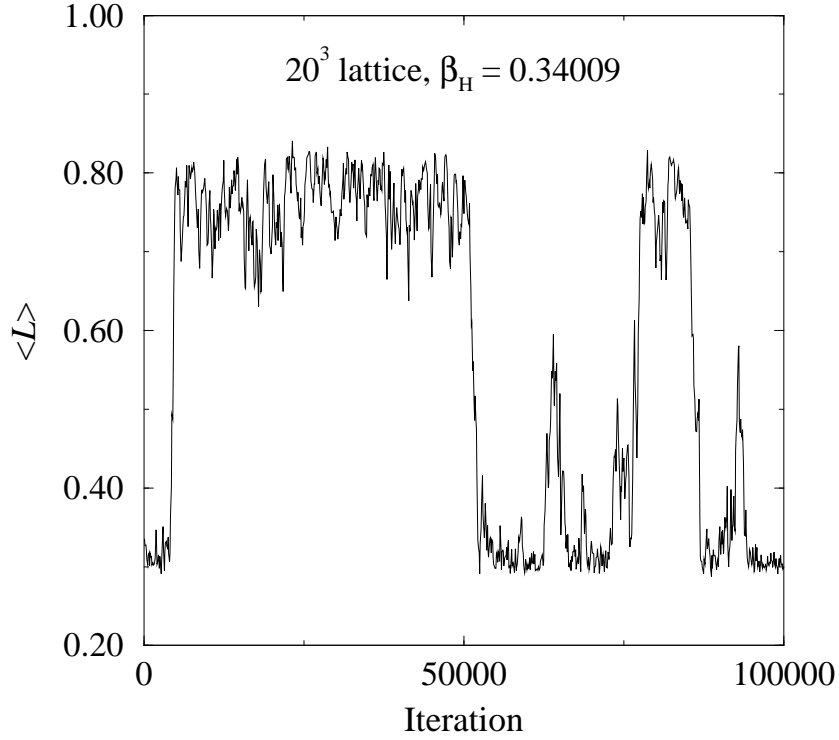


Figure 3: The Monte Carlo time history of the lattice simulations for $m_H = 35$ GeV on a 20^3 lattice near critical β_H .

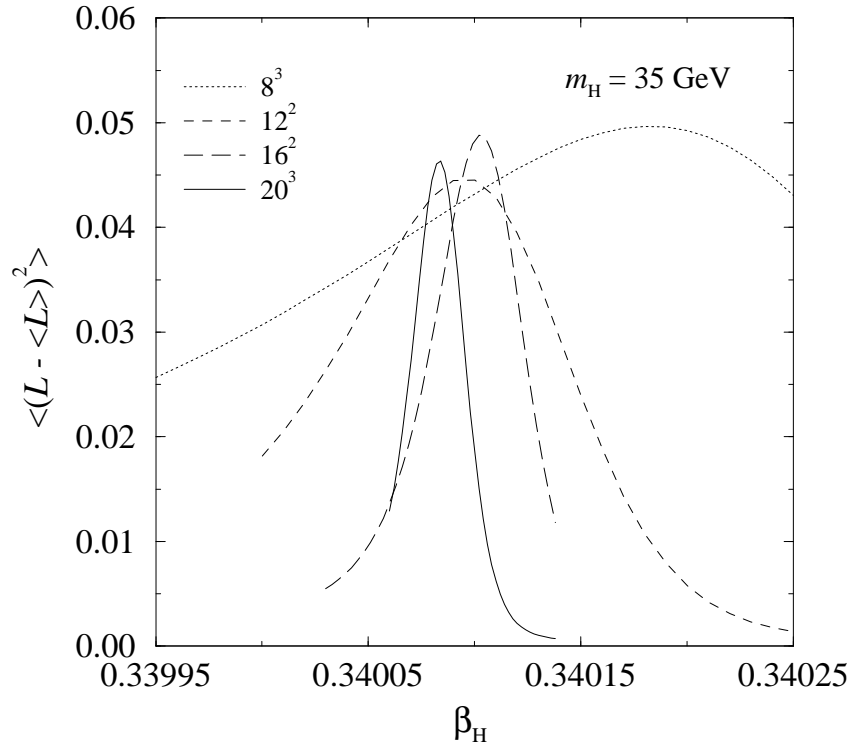


Figure 4: The dependence of the second moment of the order parameter L on β_H for different lattice sizes and $m_H = 35$ GeV.

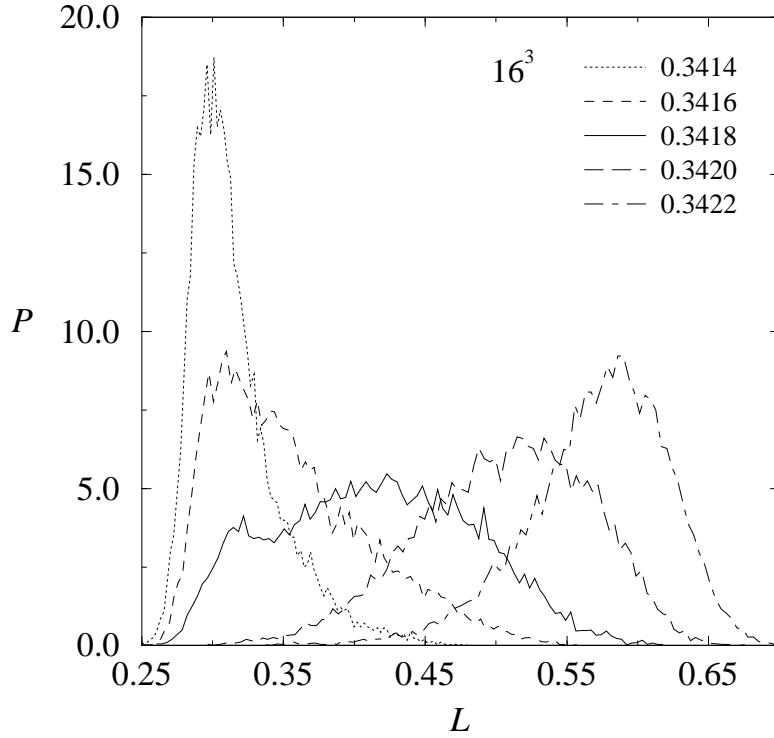


Figure 5: The distribution of $L = \text{Tr} V^\dagger(\mathbf{x})U_i(\mathbf{x})V(\mathbf{x} + i)$ for $m_H = 80$ GeV and a 16^3 lattice for different values of β_H .

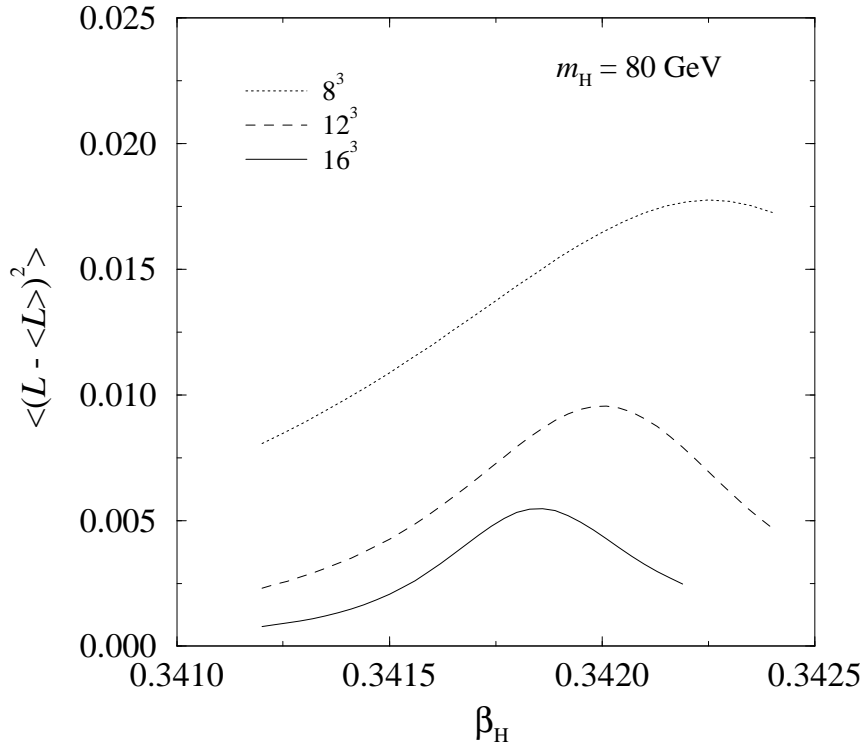


Figure 6: The dependence of the second moment of the order parameter L on β_H for different lattice sizes and $m_H = 80$ GeV.

This figure "fig1-1.png" is available in "png" format from:

<http://arxiv.org/ps/hep-ph/9305345v1>

This figure "fig2-1.png" is available in "png" format from:

<http://arxiv.org/ps/hep-ph/9305345v1>

This figure "fig3-1.png" is available in "png" format from:

<http://arxiv.org/ps/hep-ph/9305345v1>

This figure "fig4-1.png" is available in "png" format from:

<http://arxiv.org/ps/hep-ph/9305345v1>

This figure "fig5-1.png" is available in "png" format from:

<http://arxiv.org/ps/hep-ph/9305345v1>

This figure "fig6-1.png" is available in "png" format from:

<http://arxiv.org/ps/hep-ph/9305345v1>